

A simplified pseudo-static seismic analysis of reinforced soil walls with uniform surcharge

S.N. Moghaddas Tafreshi^{1,*}, T. Nouri A²

Received: July 2012, Revised: May 2013, Accepted: July 2013

Abstract

This paper presents a simple solution based on the limit equilibrium of sliding soil wedge of reinforced backfill subjected to the horizontal acceleration in the framework of the pseudo-static method. In particular, contrary to most studies on the reinforced retaining wall, the solution proposed in this study, takes into account the effect of the uniform surcharge on the reinforced backfill soil and of its distance from the face of the wall. The results are investigated in dimensionless form of the maximum reinforcement required strength (K_{max}), the dimension of the sliding wedge (L_c/H), and the factor of safety (FS). Compared to the reinforced backfill without surcharge, the presence of surcharge over the reinforced backfill and of its distance from the top of the backfill have significant effects on the stability of the system. For a fixed surcharge, a minimum distance of surcharge exists for which the presence of the surcharge does not affect the solution and the failure mechanism is that corresponding to the case of system with no surcharge. A detailed design example is included to illustrate usage of proposed procedures. Comparisons of the present results with available results show a favorable agreement.

Keywords: Seismic design, Reinforced backfill, Pseudo-static analysis, surcharge, safety factor.

1. Introduction

During an earthquake, significant damage can result due to instability of the soil in the area affected by internal seismic waves. In addition, loss of soil strength during earthquake can initiate movement of large blocks of soil, known as lateral displacement, which can result in extensive damage to utilities. In the last decades, the research on seismic stability of unreinforced soil structures by limit equilibrium method has popularity gained due to their inherent advantage over the conventional retaining walls in performance [1-5]. Caltabiano et al. [1] used the pseudo-static methods for unreinforced soil-retaining walls under seismic condition. Their solution considered the effect of the presence of the wall and uniform surcharge on the backfill. They found that the system will collapse for a lower seismic acceleration and with a larger inclination of the failure wedge than the case of the system without surcharge. More recently, for the seismic analysis, analytical derivations of the expression for the total dynamic active thrust [5] and total dynamic passive pressure [6] on the unreinforced retaining wall from the

cohesive-frictional soil backfill considering both horizontal and vertical seismic coefficients has been presented.

Due to technical and economical advantage of soil reinforcement, geosynthetic-reinforced soil is gaining considerable attention in geotechnical applications [e.g., 7, 8]. The reinforced soil-walls provide a valuable alternative to traditional concrete and masonry walls. No footing of any kind is required in the case of reinforced soil-walls, and the lowest reinforcement layer is placed directly on the foundation soil. Hence, the use of reinforced soil walls and slopes is extensively growing [e.g., 9-20]. Ling and Leshchinsky [10] investigated the effect of both vertical and horizontal accelerations on the seismic design of geosynthetic reinforced soil wall include the required strength and length of reinforcement layers. Nouri et al. [14] used horizontal slice method (HSM) to evaluate the effects of the horizontal and vertical acceleration values and amplification of pseudo-static acceleration on reinforced soil slopes and walls. Narasimha et al. [15] studied the effect of oblique displacement on safety factor of reinforced wall using HSM in pseudo-static analysis. Vieira et al. [17] presents results from a developed computer program, based on limit equilibrium calculations, able to calculate earth pressure coefficients for static and seismic loading conditions, assuming distinct failure mechanisms and earth pressure distributions. Shahgholi et al. [18] using horizontal slice method (HSM) and assuming multi-linear failure plane determined the required tensile force generated in a reinforced soil wall

* Corresponding author: nas_moghaddas@kntu.ac.ir

¹ Professor, Department of Civil Engineering, K.N. Toosi University of Technology, Valiasr St., Mirdamad Cr., Tehran, Iran

² Msc graduated, Dept. of Civil Engineering, K.N. Toosi University of Technology, Tehran. Iran

subjected to both horizontal and vertical seismic forces. Ahmadabadi and Ghanbari [19] suggested a new approach to determine the active earth pressure on retaining walls with reinforced and unreinforced cohesive-frictional backfill based on the horizontal slices method. They showed that the angle of failure wedge for cohesive-frictional soils increases linearly with an increase in the cohesive strength of the soil.

Most previous works were mostly limited to either unreinforced soil walls with/without surcharge or to reinforced soil walls with no surcharge. Hence, in this paper an attempt is made to propose a closed-form approach of modified limit equilibrium of the sliding soil wedge of the reinforced backfill with uniform surcharge based on pseudo-static analysis. The effect of horizontal coefficient acceleration, friction angle of soil, interface friction angle of soil and reinforcement; length and number of reinforcement layers, and particularly, the effect of uniform surcharge and its distance from the face of the wall are considered on the internal stability of reinforced soil walls. The internal design of reinforced soil walls and slope is determination of the maximum dimensionless form of strength of reinforcement layers (K_{max}), the dimension of the sliding wedge (L_c/H), and the safety factor of reinforcement layers (FS) due to axial pullout of reinforcement layers.

It should be noted that, design based on pseudo-static analyses are, frequently, considered conservative since the transitory earthquake acceleration assumes to act permanently as a static force in the structure. However, this conservatism may compensate the possible acceleration amplification that has not implicitly been considered in the design [9, 17].

2. Proposed Methodology

Fig. 1 shows a reinforced soil wall of height, H , with reinforcement of length, L_r , in a backfill with angle of friction, ϕ and with unit weight, γ . The backfill is reinforced with "n" layers of planar reinforcement and is subjected to the uniform surcharge q , at a certain distance from the wall, λH . The spacing between the reinforcement layers is $S_v=H/n$, except for the top and bottom layers of reinforcement which have spacing of $S_v/2$.

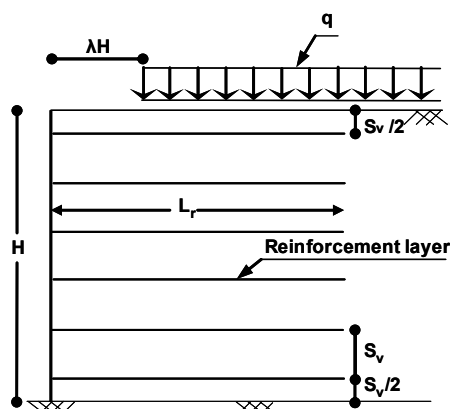


Fig. 1 Sketch of the reinforced soil-wall system with surcharge

Pseudo-static methods extend conventional limit-equilibrium methods of analysis for earth structures to include destabilizing body forces. A simple pseudo-static approach, proposed by Caltabiano et al. [1] has been developed, here in this paper. They used pseudo-static approach for unreinforced soil retaining wall with surcharge under horizontal seismic condition. The main advantage of the current research compared with Caltabiano et al. [1] is, the investigation and analysis of the seismic stability of reinforced soil-wall system with uniform surcharge which has not been investigated by Caltabiano et al. [1]. The assumptions made in this analysis are described the following:

- the soil is homogeneous, isotropic, dry and cohesionless;
- the unstable wedge slides directly downward from the former to the latter condition;
- the uniform surcharge is applied to a certain distance from the top of the wall;
- the seismic action is constant at any instant, in the whole soil-mass-wall;
- the soil-wall system is long enough for the end effects to be neglected (plane-strain conditions);
- the failure wedge is a plane; regardless of the reinforcement provision;
- full mobilization of shear resistance is considered along the sheet-soil interfaces; and
- safety factor considered due to axial pullout of reinforcement layers
- The unstable wedge slides directly downward from the former to the latter condition. Choudhury and Ahmad [16] in calculating the reinforced-soil wall showed, of two possible failure modes, direct sliding and overturning modes, direct sliding is the critical one and thus needs to be given due consideration.

Similar to the most studies [12,14,15], the effect of facing system is not considered - i.e., the inertia force of the wall face is ignored and the results of the study are valid for relatively low mass facings and may not be applicable to some modular block wall systems. On the other hand, the stability analyses were conducted for a flexible geosynthetic reinforced slope with a wrap around face and the effect of the facing elements was neglected. Thus, the analytical formulation is consistent with the flexible behaviour of a reinforced wall or slope.

Although, the results of laboratory shaking-table tests on models of reinforced slopes with an inclined facing have shown the most frequently observed failure plane during a seismic event, are either a log-spiral failure surface/bi-linear failure surface [21], but for steep reinforced slopes and vertical reinforced wall, failure plane degenerates to a planar failure [12]. Hence, the failure plane is considered independent of the provision of reinforcement [22], inclined at an angle of α (planar rupture surface AB in Fig. 2), with respect to the horizontal [15]. Basha and Babu [23] (2009) reported the planar failure surface to investigate external stability of reinforced wall with a uniform surcharge over the whole retained surface using a pseudo-dynamic approach. Ghanbari and Taheri [24] used the planar failure surface to

investigate active earth pressure in reinforced retaining walls subject to a line surcharge. However, although, Nimbalkar et al. [12] and Nouri et al. [14] showed that for the vertical reinforced wall, failure plane degenerates to a planar failure, the possibility of non-linear failure wedge due to surcharge could be investigated in the future studies.

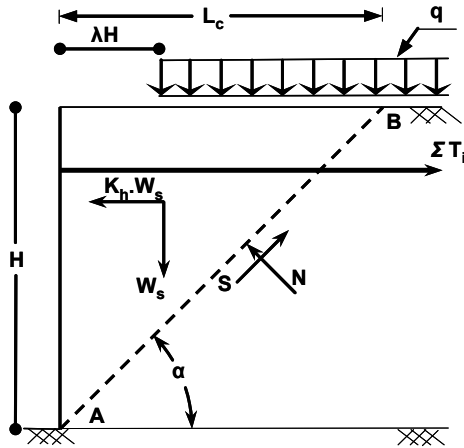


Fig. 2 Forces acting on the wedge failed of reinforced soil-wall system

2.1. Critical failure plane; α_{cri} and maximum total tensile force generated in the reinforcements; K_{max}

During earthquake the reinforced soil-wall system may either move together with the ground or move relatively respect to the ground. These two conditions are referred to as absolute motion and relative motion, respectively; the system shifting from the former to the latter condition depends on the value of the seismic horizontal acceleration $a_h = k_h g$ which k_h , and g are the horizontal seismic coefficient and gravity acceleration, respectively.

The free body diagram of the failure wedge and its acting forces, are schematically shown in Fig. 2. In this figure, S and N are the shear (tangential) and normal forces

acting on the failure plane, respectively. $\sum_{i=1}^n T_i$ is the sum of the forces needed to maintain the stability of the reinforced retaining wall, T_i is the tension force generated in the i^{th} reinforcement layer located at the soil failure wedge horizontally and n is the number of reinforcements.

The dynamic equilibrium conditions for the whole failure wedge in X and Y directions are given in Eqs. (1) and (2); respectively. Note that the effect of the seismic acceleration on the surcharge, q is considered in Eq. (1) and (2), and Fig. 2 by considering the effect of surcharge, q , on the weight of the soil failure wedge, W_s in Eq. (5).

$$\sum F_x = 0 \text{ (for the whole system)}$$

i.e.,

$$S \cos \alpha - N \sin \alpha - k_h W_s + \sum_{i=1}^n T_i = 0 \quad (1)$$

$$\sum F_y = 0 \text{ (for the whole system)}$$

i.e.,

$$S \sin \alpha + N \cos \alpha - W_s = 0 \quad (2)$$

The shear force S on the failure plane is defined as:

$$S = N \tan \phi \quad (3)$$

Eqs. (1), (2), and (3) can be solved, simultaneously, and so, the dynamic equilibrium condition obtains by the following expression:

$$\sum_{i=1}^n T_i = W_s \cdot [k_h + \tan \phi (\alpha - \phi)] \quad (4)$$

The value of W_s can be written as follow:

$$W_s = \frac{\gamma H^2}{2} \left(\frac{1}{\tan \alpha} - \frac{2q\lambda}{\gamma H} \right) + \frac{qH}{\tan \alpha} \quad (5)$$

Introducing Eq. (5), and after simple calculation, Eq. (4) becomes:

$$K (1 + Y \Phi) Y - [1 + Q (1 - \lambda Y)] [k_h (1 + Y \Phi) + (Y - \Phi)] = 0 \quad (6)$$

Where $K = 2 \sum T_i / \gamma H^2$, $Q = 2q / \gamma H$, $Y = \tan \alpha$ and $\Phi = \tan \phi$ are all dimensionless quantities. Eq. (5) can be solved with respect to K :

$$K = \frac{[1 + Q (1 - \lambda Y)] \{k_h (1 + Y \Phi) + (Y - \Phi)\}}{(1 + Y \Phi) Y} \quad (7)$$

2.2. Safety factor, FS: Bond resistance due to axial pullout of reinforcement

Fig. 3a shows the arrangement of layers of reinforcement, their length, L_r and their spacing, S_v . The parameters of $L_i = L_r - (H - z_i) \cot \alpha_{cri}$ and $L'_i = (H - z_i) \cot \alpha_{cri}$ are the effective length of i^{th} layer of reinforcement beyond the critical failure plane and located at the critical failure plane, respectively. The parameter of $z_i = (i - 0.5) S_v$ is the embedment depth of i^{th} layer of reinforcement from the top and t_i is due to bond resistance force mobilized in the i^{th} reinforcement layers over the effective length of reinforcement, L_i .

Calculating of safety factor is carried out assuming full mobilization of shear resistance along the reinforcement sheet-soil interfaces. The shear resistance is considered only due to axial pullout of reinforcement. The sum destabilizing acting force in a reinforced soil wall is resisted by the sum tension mobilized, $\sum_{i=1}^n t_i$ in the reinforcement layers over the effective length of reinforcement, L_i in the stable soil mass. The value of

Table 1 Geometric and design parameters used for reinforced retaining wall.

Description	Value
Height of the wall; H (m)	5 m
Unit weight of the soil; γ (kN/m ³)	18
Internal angle of soil friction; ϕ (degree)	25, 30, 35, 40
Soil cohesion; c	0
Uniform surcharge distributed; q (kPa) in terms of non-dimensional parameter, Q	0, 11.25, 22.5, 33.75, 45 ($Q=0, 0.25, 0.5, 0.75, 1$)
Normalized certain distance from the top of the wall, λ	0, 0.2, 0.4, 0.6, 0.8, 1, 1.2, 1.4, 1.6, 1.8, 2
Reinforcement length, L_r (m) in terms of non-dimensional parameter, L_r/H	0.4, 0.6, 0.8, 1.0, 1.2
Coefficient of seismic horizontal acceleration; k_h	0.0, 0.1, 0.2, 0.3

3.2. The effect of the normalized surcharge; Q and the normalized distance; λ of the surcharge

Fig. 4 and Fig. 5 show respectively the variation of K_{max} and L_c/H as a function of λ and Q for different values of k_h and for $\phi=30^\circ$. From Fig. 4, it observes that for a certain value of λ with increase in the value of Q , the value of K_{max} increases, regardless of the coefficient of horizontal acceleration value. In addition, it is apparent that for a given value of Q and k_h the value of K_{max} decreases with increasing λ until a limit is reached

($\lambda=\lambda_{min}$). When the surcharge is far enough from the wall, an increase in value of λ has no effect on the K_{max} value and its value is that of the system with no surcharge (the curves intercept the horizontal line in Fig. 4a-d for $Q=0$). Consequently, it is possible to verify that for a fixed surcharge and for a fixed acceleration a minimum distance λ_{min} exists, for which the presence of the surcharge does not affect the value of K_{max} . In other terms, for $\lambda \geq \lambda_{min}$, the value of K_{max} would result a constant value corresponding to the system without surcharge.

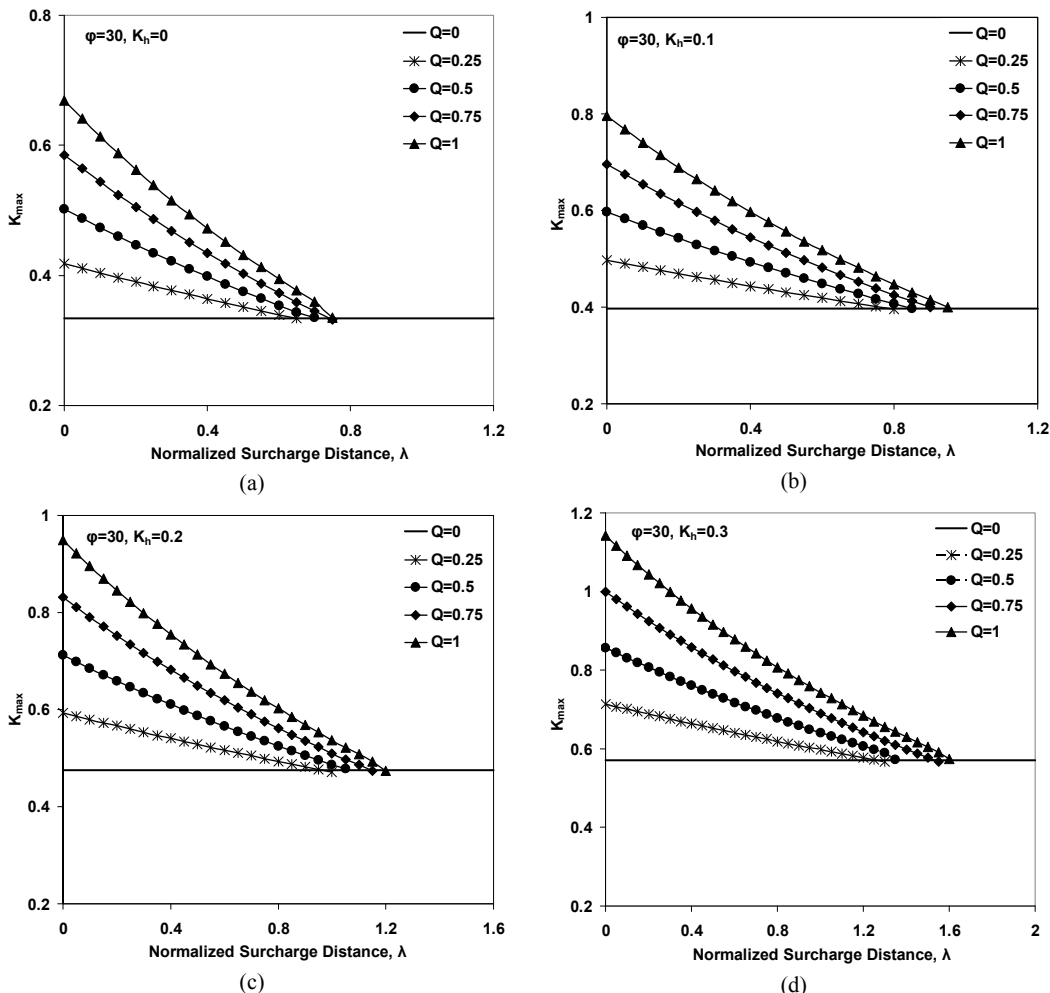


Fig. 4 Variation of K_{max} with λ for different values of Q and for different values of k_h (a) $k_h=0$, (b) $k_h=0.1$, (c) $k_h=0.2$ and (d) $k_h=0.3$

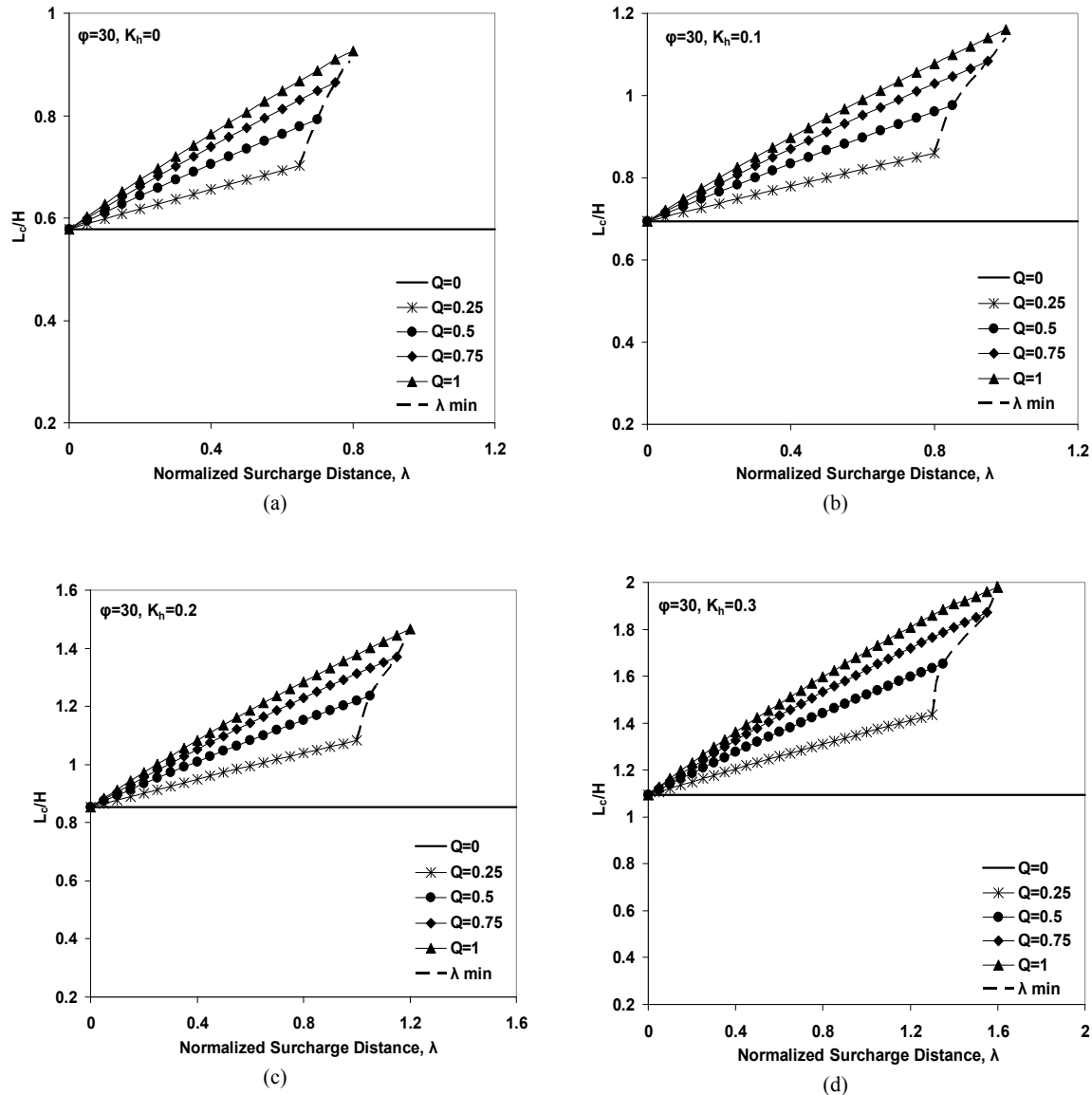


Fig. 5 Variation of L_c/H with λ for different values of Q and for different values of k_h (a) $k_h=0$, (b) $k_h=0.1$, (c) $k_h=0.2$ and (d) $k_h=0.3$

Likewise, Fig. 5 shows for a given value of Q , the value of L_c/H increases (i.e. the failure wedge angle with respect to the horizontal decreases) with increasing the value of λ until a limit value ($\lambda=\lambda_{min}$) is reached. The dashed curves in Fig. 5 show the envelope values of $\lambda=\lambda_{min}$, which after that the failure wedge does not expand. In particular, Fig. 4 and Fig. 5 show that the existence of surcharge near the wall, increases the value of K_{max} (Fig. 4), but it can prevent of expanding the failure zone (Fig. 5). It can be attributed to the confining pressure that caused due to existence of the surcharge on the failure zone. For a given k_h when the surcharge located at $\lambda=0$, the size of failure wedge remains constant (Fig. 5), regardless of the magnitude of surcharge, whereas the value of K_{max} (Fig. 4) increases due to increase in the surcharge value. In

the case of $k_h=0$ (Fig. 5a), when the surcharge located at $\lambda=0$ the failure plane inclination, α is 60° ($L_c/H=0.577$). This value of α confirms the failure plane inclination of $(\pi/4+\varphi/2)$ in accordance with Coulomb theory.

In order to investigate clearly the effect of surcharge and its distance from the face of wall, the variation of λ_{min} with Q for different values of k_h and for different values of φ is shown in Fig. 6. These curves provide the minimum distance of surcharge from the top of the wall, λ_{min} to ignore the effect of surcharge on the value of K_{max} and L_c/H . The value of λ_{min} for a fixed surcharge, Q and for a fixed acceleration coefficient, k_h extracted from Fig. 4. From this figure, it may be clearly observed that the value of λ_{min} increases with increase in the value of surcharge, irrespective of the values of k_h and φ .

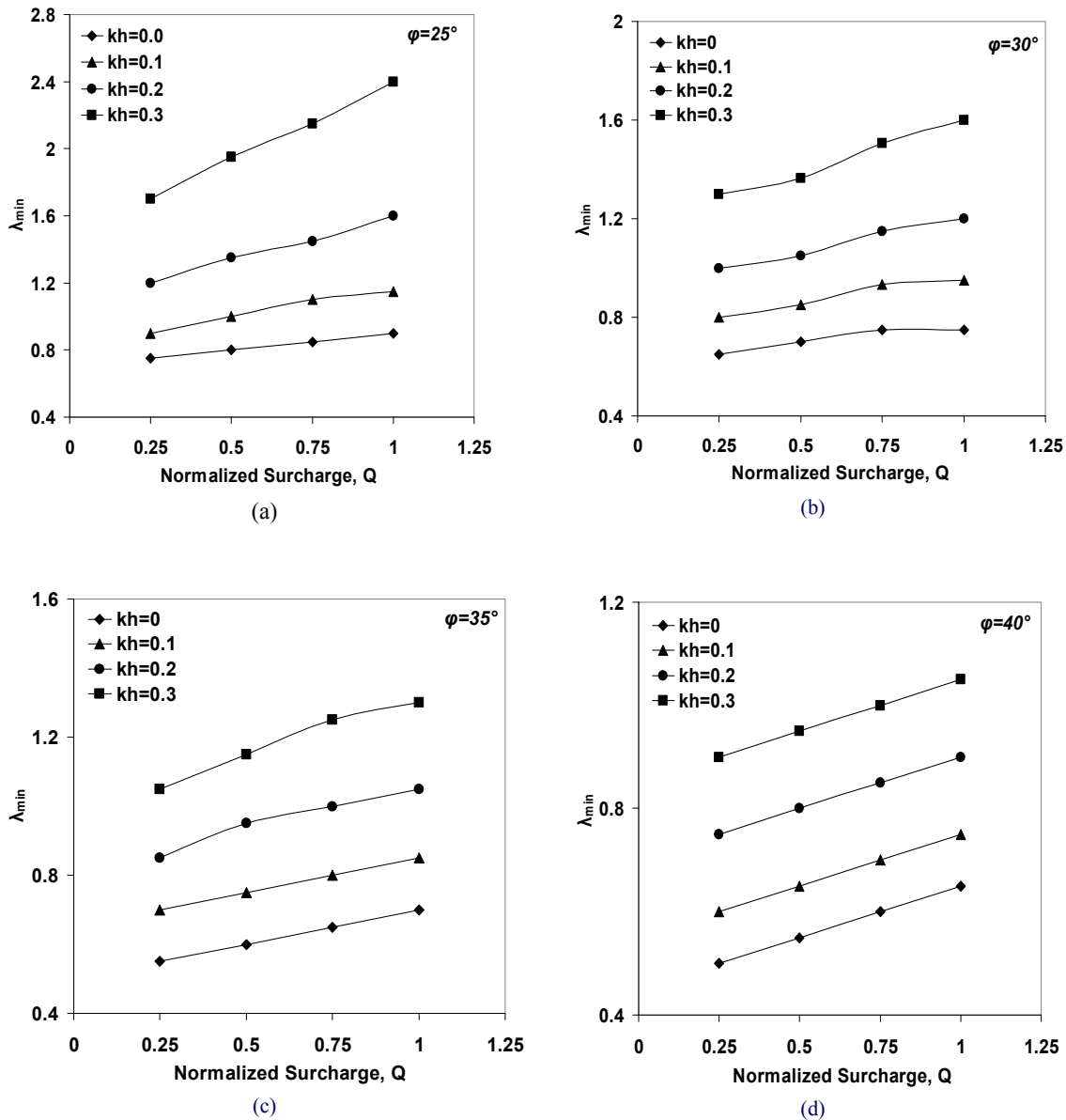


Fig. 6 Variation of λ_{min} with Q for different values of k_h and for different values of ϕ (a) $\phi=25^\circ$, (b) $\phi=30^\circ$, (c) $\phi=35^\circ$, and (d) $\phi=40^\circ$

Also, for a given value of Q , the value of λ_{min} increases with increase in the k_h value, regardless of soil friction angle, ϕ . The positive effects of ϕ in decreasing the value of λ_{min} clearly observe in Fig 6a-d. It implies that the value of λ_{min} significantly decreases with increase in the ϕ value. For example, for $k_h=0.2$, the λ_{min} of 1.31, 1.06, 0.9, and 0.775 needs to be ignored the effect of normalized surcharge of 0.5 ($Q=0.5$), respectively for the ϕ value of 25° , 30° , 35° , and 40° . Also this figure shows that, for a fixed k_h value, the surcharge lies beyond the extension of the failure wedge will affect the value of K_{max} only if its intensity is sufficiently large. In other words, if the surcharge is far from the wall top, only large values of the surcharge, Q or high values of seismic acceleration

coefficient, k_h are able to affect the failure plane and the value of K_{max} .

Fig. 7 shows the variation of K_{max} and L_c/H with normalized surcharge, Q located at $\lambda=0.4$ for $\phi=30^\circ$ and for different values of k_h . It is of interest to note that the value of K_{max} steadily, approximately linear, increases with respect to the Q value. The value of K_{max} increases as compared to that obtained corresponding to the system without surcharge. For example, for k_h value of 0.3, 0.2, 0.1, and 0, the value of $K_{max}=0.57$ would be needed, respectively for Q of 0, 0.36, 0.875 and 1.639. It reveals with increase in the intensity of surcharge acting on the backfill, a soil-wall system would be collapsed by the lower value of k_h .

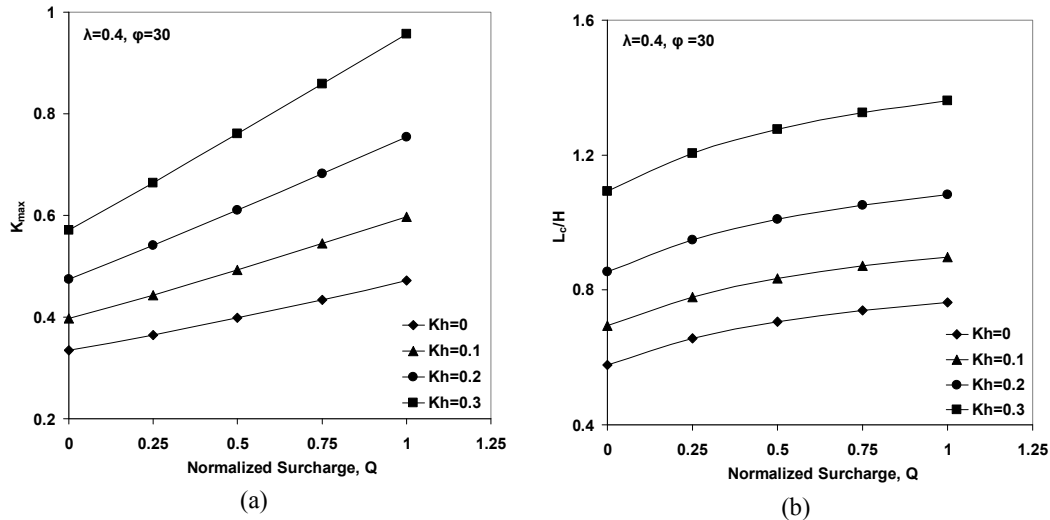


Fig. 7 Variation of K_{max} and L_c/H with Q for different values of k_h (a) K_{max} and (b) L_c/H

Fig. 7b indicates that the value of L_c/H (i.e. the size of failure wedge) increases with respect to the Q value (or the angle between failure surface and horizontal plan decreases), irrespective of the magnitudes of the k_h values. Furthermore, this figure shows that the rate of enhancement in the value of L_c/H can also be seen to reduce as no marked further increase in the size of failure wedge would be expected when the Q value increases to more than 1 ($Q > 1$). In addition, Fig. 7b shows that the specified L_c/H would be produced due to the lower value

of the k_h when the surcharge intensity increases.

Fig. 8a shows the variation of factor of safety, FS with Q for different value of k_h and, for $\phi = 30^\circ$, $\phi_r = 2/3\phi = 20^\circ$, $n = 5$, $L_r/H = 0.8$, and $\lambda = 0.4$. It shows the value of FS decreases with increase in the intensity of surcharge acting on the backfill, Q . The decrease in FS value shows more enhancement in the $\sum_{i=1}^n T_i$ compared to $\sum_{i=1}^n t_i$ with increase in the surcharge value.

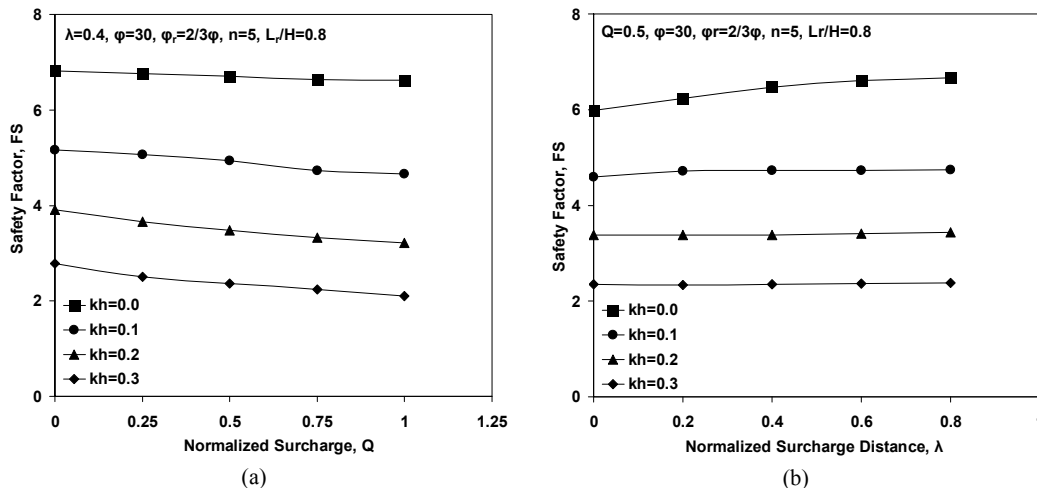


Fig. 8 Variation of FS with different values of (a) normalized surcharge, Q and (b) normalized surcharge distance, λ for different values of k_h

The variations of FS with λ for different values of k_h , and for $\phi = 30^\circ$, $\phi_r = 2/3\phi = 20^\circ$, $n = 5$, $L_r/H = 0.8$, and $Q = 0.5$ is the subject of Fig. 8b. This figure depicts that the increase in the value of λ is not significantly affected the value of FS , particularly, in the case of nonzero value of k_h . The insignificant increase in FS value could be attributed to the reduction in both the $\sum_{i=1}^n t_i$ and $\sum_{i=1}^n T_i$ with increase in the surcharge distance, λH .

However, the results presented here emphasize that a

proper attention must be paid to determine the effect of Q and λ on the values of K_{max} , L_c/H (L_r/H) and FS , as a significant reduction in stability of wall under seismic loads may lead to the catastrophic failure.

3.3. The effect of the horizontal seismic acceleration, k_h and the angle of friction, ϕ on K_{max} and factor of safety

The variation of K_{max} with horizontal seismic coefficient, k_h for five different angle of friction, $\phi = 25, 30$,

35, 40, 45, and for normalized surcharge of 0.5 ($Q=0.5$) located at $\lambda=0.4$ are shown in Fig. 9. The normalized surcharge of $Q=0.5$ provides the surcharge of $q=22.5$ kN/m² (it is about 1.2 m thickness of backfill on the reinforced retaining wall). Fig. 9 reveals that the values of K_{max} significantly increase with increase in horizontal seismic coefficient, k_h , irrespective of the value of φ . For a typical value of $\varphi=35$, the values of K_{max} are about 0.31, 0.40, 0.50, and 0.62, respectively for k_h of 0, 0.1, 0.2, and 0.3. The increase in K_{max} value with k_h is attributed to a large failure soil acting at the back of reinforced soil (the active soil wedge behind the wall) as the coefficient increases (9, 28].

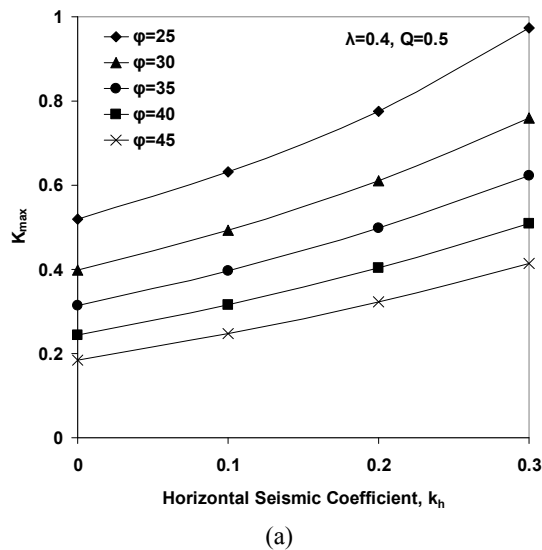


Fig. 9 Variation of K_{max} with horizontal seismic coefficient, k_h for different soil internal angle of friction, φ

Besides, this figure depicts that, an increase in the soil internal angle of friction; φ considerably decreases K_{max} value, irrespective of k_h value. For example, for $k_h=0.2$, the values of K_{max} is 0.78 when $\varphi=25$, but reduces to about 0.40 when $\varphi=40$. Although, it apparently seems a simple result, but this is an important conclusion, which indicates the soil shear strength, φ plays an important role and must be carefully, selected in practical design.

To investigate the effect of soil internal angle of friction, φ and horizontal seismic coefficient, k_h on the values of safety factor, FS , the variation of FS with k_h for different soil internal angle of friction, φ and for $n=5$, $L_r/H=0.8$, $\lambda=0.4$, $\varphi_r=2/3\varphi=20^\circ$, and $Q=0.5$ is shown in Fig. 10. This figure depicts the value of FS considerably decreases non-linearly, particularly for high values of angle of friction ($\varphi \geq 35^\circ$), with an increase in horizontal seismic coefficient, k_h owing to an increase in the destabilizing force. It is interesting to note that for a given value of φ , the rate of decrease in FS value is greater for k_h up to 0.2.

The FS value increases with an increase in the soil angle of shear resistance owing to the increase in bond resistance due to mobilization of friction resistance. Likewise, the value of FS due to increase in soil shear

strength, φ is more considerable for static loading ($k_h=0$) and low value of k_h ($k_h=0.1$) as compared with those obtained for higher value of k_h ($k_h \geq 0.2$). For example, the value of FS increases from about 4.74 to 11.64 at $k_h=0.1$ and from 2.26 to 5.93 at $k_h=0.3$ for φ increasing from 30° to 40° . The significant changes in safety factor due to change in soil shear strength, φ confirms the notability in selecting the real soil shear strength, φ in designing the reinforced retaining wall.

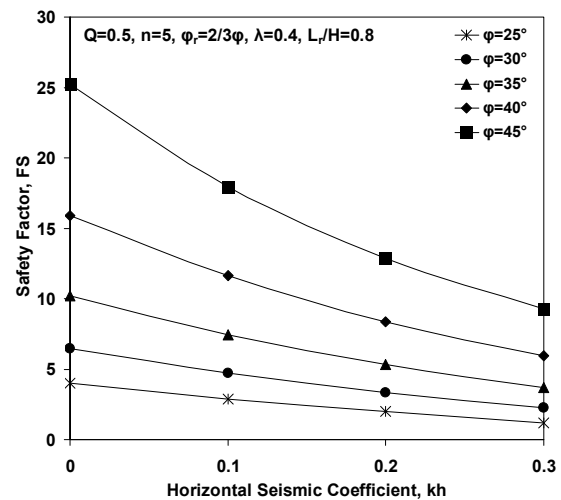


Fig. 10 Variation of FS horizontal seismic coefficient, k_h for different soil internal angle of friction, φ

In practical point of view, these results strongly emphasize that a proper attention must be paid to determine the accurate values of horizontal seismic coefficient k_h , and soil internal angle of friction, φ . On the other hand, selecting a lower value of φ and higher values of k_h than their real values may significantly increase the costs of project. Also, selecting a higher value of φ and lower values of k_h than their real values may result the catastrophic failure.

3.4. The effect of the angle of interface friction, φ_r on factor of safety

The variation of factor of safety, FS with k_h for different angles of interface friction, φ_r is the subject of Fig. 11 for $n=5$, $L_r/H=0.8$, $\varphi=30^\circ$, and normalized surcharges, $Q=0.5$ located at $\lambda=0.4$. Regardless of k_h values, factor of safety increases as the angle of interface friction increases, owing to the increase in bond resistance. It can be seen that for $k_h=0.2$, the value of FS obtained 1.61, 2.45, 3.32, 3.78, and 5.27 for the angle of interface friction, φ_r of $1/3\varphi$, $1/2\varphi$, $2/3\varphi$, $3/4\varphi$, and φ , respectively. It means the contribution of the angle of interface friction; φ_r to FS is very pronounced and needs a proper attention to the type of reinforcement and soil and to determine the accurate values of φ_r using a direct shear test and/or pullout test. Furthermore, the variation in FS for different angles of interface friction tends to decrease as the horizontal seismic coefficient increases. The effect of

horizontal seismic acceleration is more for the higher values of the angle of interface friction, φ_r . The average slope of curves for variation of k_h from 0 to 0.3 increases by about 6.8, 10.3, 14.1, 15.9, and 22.2, respectively for angle of interface friction, φ_r of $1/3\varphi$, $1/2\varphi$, $2/3\varphi$, $3/4\varphi$, and φ . Likewise, for a given value of φ_r , the decrease in absolute value of FS is lower for higher horizontal seismic accelerations. For $\varphi_r = 2/3\varphi$, when k_h changes from 0 to 0.1, FS decreases by about 1.74 unit; when k_h changes from 0.1 to 0.2, FS decreases by about 1.41 unit; and when k_h changes from 0.2 to 0.3, FS decreases by about 1.06 unit.

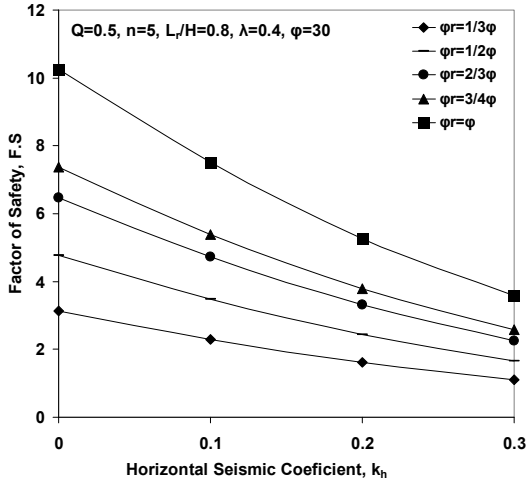


Fig. 11 Variation of FS with horizontal seismic coefficient, k_h for different angle of interface friction, φ_r .

3.5. The effect of the number reinforcement layers, n on factor of safety

Fig. 12 illustrates the variation of safety factor, FS with k_h for 3, 5, 7, and 9 layers of reinforcement, n and for $Q=0.5$, $\lambda=0.4$, $\varphi=30^\circ$, $\varphi_r=2/3\varphi=20^\circ$, and $L_r/H=0.8$. As can be seen, FS significantly decreases nonlinearly with increase in horizontal seismic coefficient. Beside, FS value increases considerably with increase in the number of reinforcement layers in the backfill, irrespective of value of k_h . It can be attributed to increase in the total bond resistance between the soil and reinforcement layers with increasing the number of reinforcement layers. From this figure, it could be easily found that the value of FS increases about 205%-210%, irrespective of value of k_h with increase in number of reinforcement layers from 3 to 9.

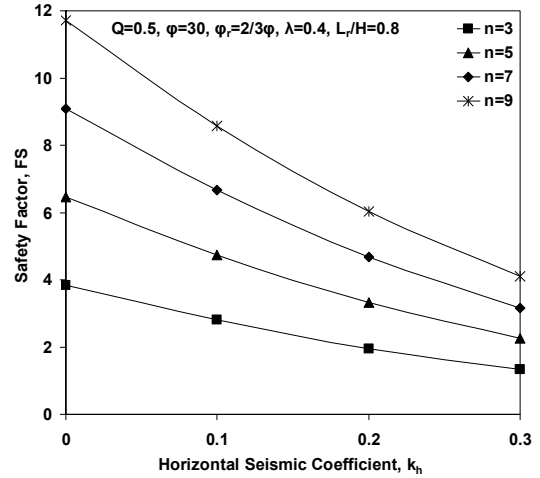


Fig. 12 Variation of FS with horizontal seismic coefficient, k_h for different number of reinforcement layers, n

3.6. The effect of the length of reinforcement layers, L_r/H on factor of safety

Variation of safety factor, FS with k_h for different length of reinforcement layers ($L_r/H=0.4, 0.6, 0.8, 1$, and 1.2) and for $Q=0.5$, $\lambda=0.4$, $\varphi=30^\circ$, $\varphi_r=2/3\varphi=20^\circ$, and $n=5$ is depicted in Fig. 13. The value of FS decreases, approximately, non-linearly with increase in horizontal seismic coefficient for different normalized lengths of reinforcement, L_r/H and increase proportionately with increase in L_r/H ratio. The increase in factors of safety with increasing length of the reinforcement, L_r/H is due to increase in bond resistance between the soil and reinforcement layers. For example, for $k_h=0.1$, the increase in FS is about 225% (FS varies from 2.80 to 9.06) and for $k_h=0.3$, the increase in FS is about 270% (FS varies from 1.28 to 4.75) with increase in the value of L_r/H ratio from 0.6 to 1.2. For the parameters given in Fig. 13, the comparative investigations imply that in order to achieve a minimum value in safety factor, FS of 1.5 ($FS \geq 1.5$) the length of reinforcement layers, L_r must be selected between 0.6-0.8 times of the height of reinforced soil wall, H , irrespective of horizontal seismic coefficient.

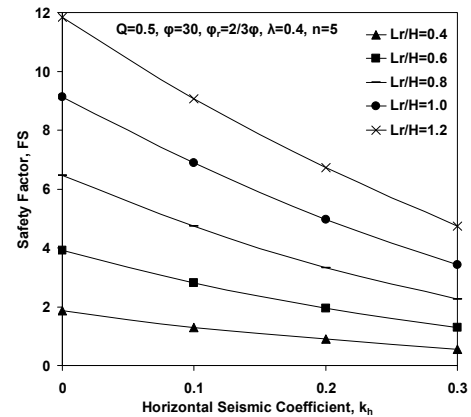


Fig. 13 Variation of FS with horizontal seismic coefficient, k_h for different length of reinforcement layers, L_r/H

4. Comparison of Results with Other Studies

No experimental and analytical data on the internal stability of reinforced soil walls subjected to uniform surcharge with the exact match conditions were available to compare with the results of the current approach. So, in order to study the validity of presented formulation, the results have been compared with the available results at the same condition as follows:

- (1) In the case of unreinforced wall with uniform surcharge ($Q \neq 0$ and $\lambda \neq 0$), using $K=0$ in Eq (6), the limit equilibrium equation becomes:

$$[Q\lambda(1+k_h\Phi)]Y^2 + [Q\lambda(k_h - \Phi) - (1+Q)(1+k_h\Phi)]Y - (1+Q)(k_h - \Phi) = 0 \quad (11)$$

This equation is exactly similar to Eq. (6) of Caltabiano et al. [1] in the absent of gravity wall.

(2) In the case of reinforced wall without surcharge ($Q=0$), the maximum total tensile forces generated in the layers of reinforcement defined by the dimensionless parameter, K_{max} has been compared for different k_h and ϕ values in Table 2, with those for wall in pseudo static condition reported by the other researchers [10,14,15,18]. Ling et al. [10] used the Reslope program which the slip surface is assumed to be a log-spiral. Shahgholi et al. [18] considered horizontal slice method (HSM) using polylinear failure plane, whereas a linear failure plane in HSM proposed by Narasimha Reddy et al. [15]. Nouri et al. [14] used HSM with log-spiral failure surface which changed to linear failure plane in the case of vertical wall.

Table 2 Comparison of non-dimensional parameters K_{max} calculated by Ling et al. [10], HSM by Shahgholi et al. [18], HSM by Narasimha Reddy et al. [15], HSM by Nouri et al. [14], and present study with no surcharge ($Q=0$)

k_h	Ling et al. (1997)	Shahgholi et al. (2001),	Narasimha Reddy et al. (2008),	Nouri et al. (2008)	Present Study	Ling et al. (1997)	Shahgholi et al. (2001)	Narasimha Reddy et al. (2008)	Nouri et al. (2008)	Present Study
	$\phi=25^\circ$					$\phi=30^\circ$				
0	0.422	0.404	0.404	0.409	0.407	0.329	0.333	0.333	0.334	0.334
0.1	0.488	0.476	0.476	0.479	0.477	0.400	0.396	0.396	0.398	0.397
0.2	0.560	0.565	0.565	0.567	0.565	0.471	0.471	0.471	0.475	0.474
0.3	0.680	0.680	0.676	0.688	0.682	0.569	0.569	0.565	0.568	0.571
$\phi=35^\circ$					$\phi=40^\circ$					
0	0.280	0.271	0.271	0.272	0.272	0.222	0.218	0.218	0.220	0.218
0.1	0.329	0.329	0.329	0.327	0.329	0.262	0.267	0.267	0.270	0.269
0.2	0.400	0.396	0.396	0.398	0.397	0.329	0.329	0.329	0.330	0.329
0.3	0.471	0.480	0.476	0.482	0.479	0.391	0.401	0.401	0.404	0.402

Comparisons of K_{max} values from the present approach show a satisfactory agreement with those obtained from the other studies. It depicts that the bi-linear, log-spiral failure surface and two-part wedge mechanism, selected by other researchers, may not be necessary to be considered for vertical reinforced backfill.

- (3) In the case of reinforced wall with surcharge ($Q \neq 0$), the maximum total tensile forces generated in the layers of reinforcement (in terms of K_{max}) with those of Ghanbari and Taheri [24], in the static condition has been compared

for different Q and λ values in Table 3. They presented an analytical method to evaluate the stability of reinforced soil retaining walls subjected to a line surcharge. Table 3 shows a relative close match between the results of the proposed method compared with those of Ghanbari and Taheri [24]. The maximum difference in the K_{max} values for two studies was only about 13.5%. This difference might be due to difference of the type of surcharge over the reinforced wall.

Table 3 Comparison of non-dimensional parameters K_{max} calculated by Ghanbari and Taheri [24] and present study for different values of surcharge (Q) and of its distance from the face of the wall (λ) for $k_h=0$ and $\phi=30^\circ$

Surcharge value (Q)	$\lambda=0.2$		$\lambda=0.4$		$\lambda=0.6$	
	Present Study	Ghanbari and Taheri [24]	Present Study	Ghanbari and Taheri [24]	Present Study	Ghanbari and Taheri [24]
0.25	0.390	0.435	0.364	0.402	0.339	0.384
0.50	0.447	0.497	0.398	0.456	0.354	0.402

5. Conclusion

In this research, a relatively simple pseudo-static approach using a limit equilibrium method is proposed for the seismic stability of reinforced backfill with uniform surcharge set back from the wall crest. Based on the results, the following conclusions can be drawn:

1. For a surcharge located at $\lambda=0$ and for a given value

of k_h , an increase in the surcharge intensity increases the value of K_{max} , whereas the value of L_c/H remains constant.

2. For a given value of Q , k_h , and ϕ a minimum distance λ_{min} exists for which the presence of the surcharge does not affect the solution. Afterward an increase in value of λ ($\lambda \geq \lambda_{min}$) has no effect on the value of K_{max} and L_c/H . For a fixed value of k_h when the surcharge lies beyond the distance of $\lambda=\lambda_{min}$, the surcharge may be affected the

values of L_c/H and K_{max} only if the intensity of surcharge is sufficiently large.

3. For a certain value of k_h , if a surcharge places on the failure wedge ($\lambda < \lambda_{min}$ and $\lambda \neq 0$), independently of its intensity, it will affect the failure mechanism and, however, with increase in the value of Q the values of K_{max} and L_c/H increase. On the other hand, with increase in the intensity of surcharge, the soil-wall system would be collapsed by the lower value of k_h than the case of system without surcharge.

4. The value of k_h is important parameter in computing the values of K_{max} , L_c/H and FS . Furthermore, its importance increases where k_h increases ($k_h > 0.1$) and the quality of reinforced backfill decreases ($\varphi < 30$). The seismic stability of the reinforced soil wall reduces with increase in k_h , and so there is a need to provide an adequate tensile strength, length and number of reinforcement layers to maintain the desired safety levels.

5. The value of FS decreases with increase in the intensity of surcharge acting on the backfill as the rate of reduction in FS increases for higher value of k_h . The variation of FS is not significant with increase in the value of λ , particularly, in the case of nonzero k_h value.

6. The FS value increases significantly due to increase in the soil shear strength, φ , and in the angle of interface friction, φ_r . The significant changes in FS due to change in φ and φ_r emphasize on the notability in selecting the real values of φ and φ_r in designing the reinforced retaining wall.

7. Factor of safety, considerably increases with increase in the number, n and length of the reinforcement layers, L_r/H . It is due to increase in bond resistance between the soil and reinforcement layers. Overall, it could be resulted with increase in k_h and Q and also with decrease in φ and φ_r , the longer length and more number of reinforcement layers are needed.

8. Comparisons of the results of the present formulation, for the unreinforced backfill with surcharge and for the reinforced backfill without surcharge, with those obtained by the other researchers are in a good agreement. Thus, it may be safely argued that this formulation and its results may be used for designing the reinforced wall with uniform surcharged subjected to horizontal seismic loading. However, further research is needed in order to develop this method and to verify its reliability.

Note that this study investigated the internal stability of reinforced wall with surcharge, so the external stability of wall must be separately considered. Likewise, investigation a two-wedge analysis as a likely more appropriate failure surface, when the wedge is sat back from the edge of the wall, might be a fruitful avenue in future studies.

References

- [1] Caltabiano S, Cascone E, Maugeri M. Seismic stability of retaining walls with surcharge, *Soil Dynamics and Earthquake Engineering*, 2000, Nos. 5-8, Vol. 20, pp. 469-476.
- [2] Ghanbari A, Hoomaan E, Mojallal M. An analytical

method for calculating the natural frequency of retaining walls, *International Journal of Civil Engineering*, 2013, No. 1, Vol. 11, pp. 1-9.

- [3] Vieira C. A simplified approach to estimate the resultant force for the equilibrium of unstable slopes, *International Journal of Civil Engineering*, 2014, No. 1, Vol. 12, pp. 65-71.
- [4] Ghanbari A, Ahmadabadi M. Active earth pressure on inclined retaining walls in static and pseudo-Static conditions, *International Journal of Civil Engineering*, 2010, No. 2, Vol. 8, pp. 159-173.
- [5] Shukla S.K. Dynamic active thrust from $c-\varphi$ soil backfills, *Soil Dynamics and Earthquake Engineering*, 2011, No. 3, Vol. 31, pp. 526-529.
- [6] Shukla S.K, Habibi D. Dynamic passive pressure from $c-\varphi$ soil backfills, *Soil Dynamics and Earthquake Engineering*, 2011, Nos. 5-6, Vol. 31, pp. 845-848.
- [7] Abdi M.R, Sadmejad S.A, Arjomand M.A. Clay reinforcement using geogrid embedded in thin layers of sand, *International Journal of Civil Engineering*, 2009, No. 4, Vol. 7, pp. 224-235.
- [8] Asakereh A, Moghaddas Tafreshi S.N, Ghazavi M. Strip footing behavior on reinforced sand with void subjected to repeated loading, *International Journal of Civil Engineering*, 2012, No. 2, Vol. 10, pp. 139-152.
- [9] Ling H.I, Leshchinsky D. Effects of vertical acceleration on seismic design of geosynthetic-reinforced soil structures, *Geotechnique*, No. 3, Vol. 48, pp. 347-373.
- [10] Ling H.I, Leshchinsky D, Perry E.B. Seismic design and performance of geosynthetic-reinforced soil structures, *Geotechnique*, 1997, No. 5, Vol. 47, pp. 933-952.
- [11] Ausilio E, Conte E, Dente G. Seismic stability analysis of reinforced slopes, *Soil Dynamics and Earthquake Engineering*, 2000, No. 3, Vol. 19, pp. 159-72.
- [12] Nimbalkar S.S, Choudhury D, Mandal J.N. Seismic stability of reinforced soil wall by pseudo-dynamic method, *Geosynthetics International*, 2006, No. 3, Vol. 13, pp. 111-119.
- [13] El-Emam M.M, Bathurst R.J. Influence of reinforcement parameters on the seismic response of reduced-scale reinforced soil retaining walls, *Geotextiles and Geomembranes*, 2007, No. 1, Vol. 15, pp. 33-49.
- [14] Nouri H, Fagher A, Jones C.J.F.P. Evaluating the effects of the magnitude and amplification of pseudo-static acceleration on reinforced soil slopes and walls using the limit equilibrium horizontal slices method, *Geotextiles and Geomembranes*, 2008, No. 3, Vol. 26, pp. 263-278.
- [15] Narasimha Reddy G.V, Madhav M.R, Saibaba Reddy E. Pseudo-static seismic analysis of reinforced soil wall-Effect of oblique displacement, *Geotextiles and Geomembranes*, 2008, No. 2, Vol. 16, pp. 393-403.
- [16] Choudhury D, Ahmad S.M. External stability of waterfront reinforced soil structures under seismic conditions using a pseudo-static approach, *Geosynthetics International*, 2009, No. 1, Vol. 16, pp. 1-10.
- [17] Vieira C.S, Lopes M.L, Caldeira L.M. Earth pressure coefficients for design of geosynthetic reinforced soil structures, *Geotextiles and Geomembranes*, 2011, No. 5, Vol. 29, pp. 491-501.
- [18] Shahgholi M, Fagher A, Jones C.J.F.P. Horizontal slice method of analysis, *Geotechnique*, 2001, No. 10, Vol. 51, pp. 881-885.
- [19] Ahmadabadi M, Ghanbari A. New analytical procedure for seismic analysis of reinforced retaining wall with cohesive-frictional backfill, *Geosynthetics International*, 2010, No. 6, Vol. 17, pp. 364-379.
- [20] Ghanbari A, Taheri M. An analytical method for

- calculating active earth pressure in reinforced retaining walls subject to a line surcharge, *Geotextiles and Geomembranes*, 2012, Vol. 34, pp. 491-501.
- [21] Koseki, J., Bathurst, R.J., Guler, E., Kuwano, J., Mauger, M., 2006. Seismic stability of reinforced soil walls. 8th International Conference on Geosynthetics 51-77.
- [22] Kramer S.L. *Geotechnical Earth Quake Engineering*, Prentice-Hall, Upper Saddle River, NJ, 1996.
- [23] Basha B.M, Basudhar P.K. Seismic reliability assessment of external stability of reinforced soil walls using pseudo-dynamic method, *Geosynthetics International*, 2009, No. 3, Vol. 16, pp. 197-215.
- [24] Ghanbari A, Taheri M. An analytical method for calculating active earth pressure in reinforced retaining walls subject to a line surcharge, *Geotextiles and Geomembranes*, 2012, Vol. 34, pp. 1-10.
- [25] Shukla S.K. *Geosynthetics and their applications*, Thomas Telford Ltd, London, UK, 2002.
- [26] Poulos G, Davis E.H. *Elastic solutions for soil and rock mechanics*, John Wiley and Sons, Inc, New York, USA, 1974.
- [27] Math Works Inc, *MATLAB the Language of Technical Computing, Version 7.5*, Natick, MA, USA, 2007.
- [28] Bathurst R.J, Cai Z. Pseudo-static seismic analysis of geosynthetic-reinforced segmental retaining wall, *Geosynthetic International*, 1995, No. 5, Vol. 2, pp. 787-830.